Surface Tension and Density of Al−Ni Alloys

Donatella Giuranno,[†] Ausonio Tuissi,[‡] Rada Novakovic,[†] and Enrica Ricci*[,†]

Consiglio Nazionale delle Ricerche - Istituto per l'Energetica e le Interfasi, CNR IENI-GENOVA, Via De Marini, 616149 Genova (Ge), Italy, and CNR IENI-LECCO, Corso Promessi Sposi 29, 23900 Lecco (LC), Italy

In the present work, the surface tension and density of a set of Al−Ni alloys have been investigated as a function of composition and temperature. The measurements were performed by the large drop method, under equilibrium and with an oxygen-free surrounding atmosphere to prevent oxidation phenomena. The study was focused mainly on Al-rich alloys investigated in the framework of the EU FP7-IMPRESS project aimed to obtain tailor-made Al−Ni nanopowders for high-performance macroscale catalytic devices. The measured thermophysical properties were compared with both literature results and data theoretically predicted by applying thermodynamic calculation methods (e.g., QCA and CFM), with the aim to highlight the role of Al−Ni intermetallic compounds.

1. Introduction

The Al−Ni-based alloys have been expected to be used as high-temperature and oxidation-resistant materials in several fields, for example, aeronautics, turbine blade production, space systems, automotive engineering, catalytic chemistry, hydrogen fuel cell technology, and biomedicine.

In particular, Al−Ni alloys have attractive properties such as low density, high strength, and good corrosion resistance.[1]

On the basis of the Al−Ni binary phase diagram,[2] evidence is presented for five intermetallic compounds (e.g., Al_3Ni, Al_3Ni_2, Al_3Ni_5, AlNi, and $AlNi_3$). Among these intermetallics, Al_3Ni has gained considerable interest, in recent years, for catalytic applications, as a valuable alternative to the Raney-type nickel-aluminide ($Al_{68.5}Ni_{31.5}$) alloy. These catalytic materials differ from most other types of catalysts since their high surface area is achieved by selectively leaching away the aluminum with aqueous sodium hydroxide.

Recently, Al_3Ni and AlNi alloys have been extensively investigated in the framework of the EU FP7-IMPRESS project aimed to obtain tailor-made nanopowders for high-performance macroscale catalytic devices.

In spite of these attractive properties, Al−Ni based alloys have limited applications due to their extreme brittleness and the resulting difficulties in shaping and casting. For these reasons, casting and solidification modeling has become an indispensable tool in the development and optimization of Al-based alloy casting technology. However, knowledge of reliable thermophysical properties is a key issue for the modeling of industrial casting and solidification processes. The application of such numerical tools is generally hampered by a lack of reliable thermophysical property values.

Thermophysical properties can be divided into those relevant for heat and those relevant for fluid flow. The properties relevant for heat flow include the thermal conductivity, the specific heat capacity in the liquid and high-temperature solid phase, the enthalpy of fusion, and the fraction solid on cooling. The properties relevant for fluid flow include the viscosity, the density, and the surface tension together with its temperature coefficient. Moreover, knowledge of reliable surface tension and density values is important for the prediction of casting defects such as bubble entrapment and gas porosity as well as for a better understanding of the nucleation−condensation phenomena governing the production of metal nanopowders.[3]

The paucity of such reliable data is generally because of high chemical reactivity, particularly pronounced for Al-based alloys. In fact, when dealing with high-temperature surface property measurements, for example, surface tension, the values obtained in many experiments do not really refer to pure substances, but rather to alloys or solutions, especially taking into account certain surface active elements (such as oxygen) that have a dramatic effect on surface tension even if present in trace amounts.[4] The choice of an appropriate inert crucible material as well as of the proper experimental procedure in performing thermophysical property measurements, in particular those on surface tension, is the key to obtain reliable data.

In this work, an experiment-based investigation on surface tension and density behaviors of Al−Ni alloys as a function of composition and temperature is shown. Surface tension and density measurements have been performed by the large drop method.[4] On the basis of thermodynamic arguments,[5] the Al−Ni system could be affected by oxidation−evaporation phenomena. For that reason, inert crucibles have been used, and all of the measurements have been carried out under a highly reducing atmosphere.

The surface tension and density collected data show good agreement with both the few literature data available and the theoretical prediction evaluated by using the regular solution (RS) and compound formation (CFM) thermodynamic models, which allowed the role of Al−Ni intermetallic compounds to be singled out.[6]

2. Experimental Section

2.1. Sample Preparation. For this work, eight Al−Ni compositions, ranging from (11 to 98) % Al, were considered. Al_3Ni ($Al_{75}Ni_{25}$) and AlNi Raney-type ($Al_{68.5}Ni_{31.5}$) alloys were supplied by the courtesy of ACCES (Aachen-Germany), in the

* Corresponding author. E-mail: ricci@ge.ieni.cnr.it. Tel.: +390106475720. Fax +390106475700.
[†] CNR IENI-GENOVA.
[‡] CNR IENI-LECCO. E-mail: a.tuissi@ieni.cnr.it.

10.1021/je901055j
Published on Web 05/04/2010

framework of the IMPRESS project, and produced by recasting in a LINN centrifuge. The other alloys were produced at the CNR IENI laboratories. High purity (99.999 %) Ni and Al were alloyed by two different methodologies. The $Al_{97.6}Ni_{2.4}$, $Al_{92.5}Ni_{7.5}$, and $Al_{87}Ni_{13}$ alloys were prepared by induction melting from a mixture of weighed and polished small pieces of pure metals in high dense alumina crucibles. Each alloy was remelted twice under a pure static Ar atmosphere (99.9999 % Ar N60-Air Liquide) and continuous shaking of the crucible to achieve complete homogeneity. Generally, no weight loss was observed after melting. The remaining $Al_{89.7}Ni_{10.3}$, $Al_{76.5}Ni_{23.5}$, and $Al_{11.4}Ni_{88.6}$ alloys were produced by using a vacuum arc melting (VAR) furnace (Leybold LK6/45), equipped with water-cooled copper crucibles. The pure metals were alloyed under pure static Ar atmosphere at $P \approx 8 \cdot 10^4$ Pa to avoid metal vaporization effects. Small ingot buttons, of about $w = 40$ g, were produced and then remelted six times, for increasing the degree of alloy homogeneity in a noncontaminating cold hearth. The energy dispersive spectroscopy (EDS) analyses of the produced alloys in their as cast state showed chemical compositions in agreement with the nominal ones, within experimental EDS sensitivity.

2.2. Experimental Apparatus and Procedure. The measurements have been performed in an "ad hoc" designed apparatus by applying the large drop method.[4] This methodology is particularly reliable to measure the surface tension at high temperatures, giving high reproducibility. Because of the design of the sharp edges of the crucible, the liquid metal drop is pinned down at the triple line with an "apparent" contact angle much higher than the real one, so that the axis symmetry of the liquid metal drop can be imposed.

Actually, because of the high chemical reactivity characterizing the Al−Ni system, a really inert substrate material is not easily available. When dealing with such extremely reactive systems, the goal is to find a highly resistant crucible material showing, at least, negligible interactions as is the case of ZrO_2 in an under-stoichiometric state. ZrO_2 in an under-stoichiometric state is obtained by heating at $T = 1773$ K under a flowing atmosphere of Ar-5 % H_2.

Considering the higher temperature and the more enhanced evaporation phenomena and oxidation kinetics, the experiments were carried out under a fluxing atmosphere of Ar-5 % H_2 mixture. Moreover, a Zr foil placed over the liquid alloy sample has been used as a getter, to further reduce the oxygen content in the surrounding atmosphere.

The necessary cleanliness of the apparatus's environment was assured by the high quality of the materials used and a systematic procedure of baking before each experiment. A feed gas plant was also present to avoid any contamination. A high-precision flowmeter (Brooks) and microleak valve (Nupro) allowed a precise and controlled amount of gas flux inside the chamber (mean flow rate: $q = 0.8 \cdot 10^{-6}$ $m^3 \cdot s^{-1}$). The operative conditions were continuously monitored. The temperature of the samples was measured by a Pt/Pt-10 % Rh thermocouple, which was previously calibrated. During the measurements, the temperature of the sample was found to be stable within ± 2 K. The oxygen partial pressure was monitored by using two ZrO_2 oxygen sensors (μPOAS/SETNAG) with a Pd/PdO internal reference. The sensors measure the oxygen content in the feed and in the exhaust gas. The inner oxygen partial pressure, measured at the exit of the inner tube was around an average value $P < 10^{-18}$ Pa. Al−Ni alloy samples, of a mean mass $w =$ (1 to 2) g each, were mechanically abraded and chemically cleaned with organic solvents in an ultrasonic bath. The alloy sample was placed in the ZrO_2 crucible ($r = 5.5$ mm) which was laid on a sliding alumina holder of the experimental apparatus. When the apparatus conditioning (temperature, oxygen partial pressure) was reached, the sample was introduced into the center of the furnace by a pushrod magnetic manipulator. In this position the specimen, backlit by a stabilized lamp, was monitored by a charge-coupled device (CCD) camera. An optical bench allowed perfect alignment and uniformity of the light with the sample. To obtain a monochromatic light and to cut IR emissions, optical filters were interposed between the view ports of the test chamber and the CCD camera. In addition, the chamber position can be set to ensure the required horizontal alignment of both crucible and specimen. The CCD camera was equipped with standard high-quality photographic lenses. To allow measurement repeatability, the focusing, focal length, and diaphragm of the optical system were kept fixed. The acquisition frequency can be up to 10 points per second with an accuracy up to 0.1 %. The surface tension was estimated by using the nonlinear regression method proposed by Maze and Burnet.[7] The profile of the liquid drop obtained was acquired by dedicated Labview software, which is used to obtain the surface tension value in real time.[4] The magnification factor was evaluated for each image used for the surface tension measurements. The output of particular parameters and quantities, such as drop volume, density, drop weight, shape factor, contact angle, and so forth, can also be obtained. At each temperature the liquid alloy drop was allowed to equilibrate for a time $t =$ (10 to 15) min. Measurements were done only during the stepwise cooling to improve reproducibility.

The microstructure of the as-received alloy samples were examined by scanning electron microscopy (SEM) coupled with EDS analysis. After the experiments, the same investigation was applied to the top surface of solidified drops with the aim to detect oxide phases, and segregation phenomena eventually occurred.

3. Results and Discussion

3.1. Alloy Microstructure. In Figure 1, the SEM analyses of $Al_{11.4}Ni_{88.6}$ and $Al_{75}Ni_{25}$ alloys in their as cast state are shown. The EDS microanalysis performed on large areas of the $Al_{11.4}Ni_{88.6}$ sample (Figure 1a) detected a composition in agreement with the nominal one within the experimental EDS sensitivity, and a high degree of homogeneity with an absence of phase separation was observed. On the contrary, the microstructure of the $Al_{75}Ni_{25}$, depicted in Figure 1b, is characterized by the presence of three different phases: the white zones represent the phases enriched in Ni which can be identified within the λ-phase Al_3Ni_2 ($Al_{60}Ni_{40}$); the light gray ones represent the phase enriched in Al, or segregated Al, which can be identified within the κ-phase Al_3Ni ($Al_{75}Ni_{25}$); and the dark areas represent zones with a strong aluminum oxide segregation having the eutectic composition. An identical microstructure was observed for the $Al_{68.5}Ni_{31.5}$ alloy.

3.2. Surface Tension. To optimize the experimental procedure and to find a proper working atmosphere for preserving the needed "oxygen-free" conditions during the surface tension measurements, several tests were previously performed by varying the oxygen partial pressure in the surrounding atmosphere.

The surface tension behavior of $Al_{68.5}Ni_{31.5}$ as a function of temperature and oxygen partial pressure is shown in Figure 2. The experiments have been performed under two different flowing atmospheres (flow rate $q = 0.8 \cdot 10^{-6}$ $m^3 \cdot s^{-1}$): pure Ar and Ar-5 % H_2 mixture, in the temperature range $T =$ (1625 to 1725) K. A further reduction of the oxygen content was imposed

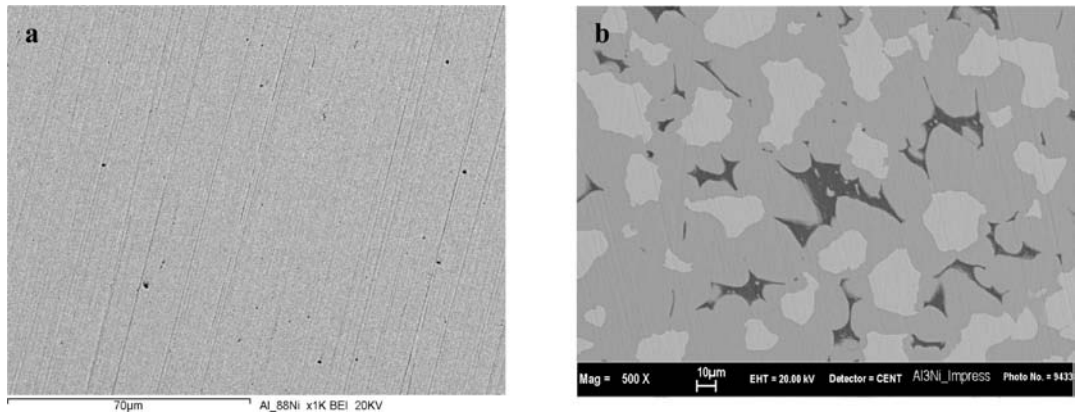

Figure 1. SEM micrographs of the as-received Al−Ni alloy sample cross sections: (a) $Al_{11.4}Ni_{88.6}$; (b) $Al_{75}Ni_{25}$. The different regions of the microstructure are described in the text.

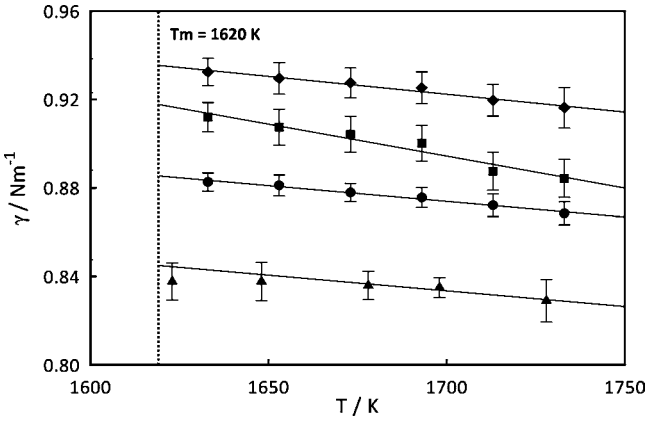

Figure 2. Measured surface tension γ of liquid $Al_{68.5}Ni_{31.5}$ alloy as a function of temperature T under: ▲, pure Ar; ●, Ar 5 % H_2; ■, pure Ar + Zr getter; ◆, Ar 5 % H_2 + Zr getter. The lines are the linear fit to the data. Dashed vertical line shows the liquidus temperature, T_L = 1620 K.

by using pure Zr as a getter. In this case, the oxygen partial pressure was defined by the chemical equilibrium of the Zr oxidation reaction.[5] Then, the oxygen partial pressures imposed during the four different experimental runs were the following: pure Ar, $P_{O2} = (10^{-2}$ to $10^{-1})$ Pa; pure Ar + Zr getter, $P_{O2} = (10^{-19}$ to $10^{-18})$ Pa; Ar-5 % H_2 mixture, $P_{O2} = (10^{-21}$ to $10^{-20})$ Pa; Ar-5 % H_2 mixture + Zr getter, $P_{O2} < 10^{-21}$ Pa.

The different oxygen content resulted in a different surface tension behavior: the lowest surface tension values were obtained under the more "oxidizing" atmosphere (pure Ar),

Table 1. Surface Tension γ_L and Surface Tension Temperature Coefficient γ' of Al−Ni Alloys Calculated at the Liquidus Temperature T_L and Measurement Temperature Range

alloy	T_L / K	γ_L / N·m^{-1}	$\gamma' \cdot 10^{-3}$ / N·m^{-1}·K^{-1}	T range / K
$Al_{97.6}Ni_{2.4}$	913	0.830 ± 0.004	−0.110	1053 to 1123
$Al_{92.5}Ni_{7.5}$	1043	0.875 ± 0.004	−0.185	1123 to 1233
$Al_{89.7}Ni_{10.3}$	1073	1.070 ± 0.006	−0.360	1348 to 1434
$Al_{87}Ni_{13}$	1123	0.847 ± 0.004	−0.085	1173 to 1273
$Al_{76.5}Ni_{23.5}$	1343	1.030 ± 0.002	−0.515	1418 to 1476
$Al_{75}Ni_{25}$	1398	0.906 ± 0.003	−0.150	1483 to 1603
$Al_{68.5}Ni_{31.5}$	1620	0.935 ± 0.007	−0.160	1633 to 1733
$Al_{11.4}Ni_{88.6}$	1713	1.781 ± 0.004	−0.402	1728 to 1783

while the highest values of surface tension have been obtained combining the oxygen reduction actions of both Ar-5 % H_2 mixture atmosphere and the gettering of Zr.

The SEM/EDS analyses (Figure 3) performed on solidified samples have confirmed the presence of a high oxygen concentration on the surface of the samples tested under pure Ar. On the other hand, the absence of oxygen on the surface of samples tested under the highest reducing atmosphere was observed. For these reasons, the atmosphere obtained by the combined action of Ar-5 % H_2 mixture and Zr was imposed as the working atmosphere during the surface tension measurements of all liquid alloys investigated. In Table 1, the experimental surface tension values (γ_L) at the liquidus temperatures (T_L) together with the temperature coefficients (γ'), obtained in this work, are shown.

The temperature dependence of surface tension of all alloys shows a linear behavior, decreasing with increasing temperature.

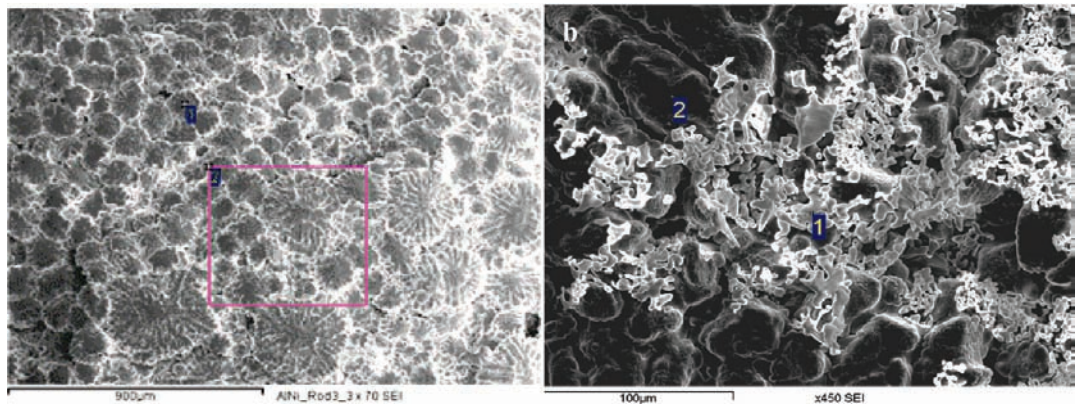

Figure 3. SEM micrographs and EDS analysis of the surface of $Al_{68.5}Ni_{31.5}$ alloy samples after the experiments under different atmospheres: (a) Ar 5 % H_2 atmosphere and Zr foil as a getter. Composition average in %: Al = 67.93; Ni = 32.07. (b) Ar atmosphere. Composition average in %: (1) O = 64.38; Al = 35.19; Ni = 0.42; (2) O = 2.40; Al = 63.89; Ni = 33.71.

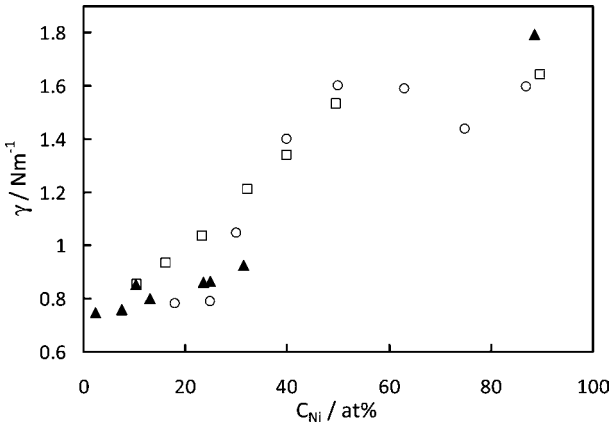

Figure 4. Composition dependence of the surface tension γ of Al−Ni alloys at $T = 1673$ K: ▲, this work; □, ref 8; ○, ref 9.

The temperature coefficients, $d\gamma/dT$, have been shown to be negative in the whole concentration range. Thus, the surface tension values increase with increasing Ni content. Because of the high temperature involved and the pronounced reactivity of the system under study, only few surface tension data are available in the literature. Ayushina et al.[8] reported the surface tension behavior of seven Al−Ni compositions measured by the sessile drop method. Egry et al.[9] measured the surface tension of eight Al−Ni compositions by the oscillating drop container-less method, deriving the surface tension data from the oscillation frequencies through the Cummings and Blackburn formalism.[10] In Figure 4, the concentration dependence of the surface tensions of Al−Ni melts measured in this work and referred to $T = 1673$ K are compared with the surface tension data reported in the literature.[8,9] For the sake of clarity, at $T = 1673$ K, the Al−Ni alloys with a Ni content higher than 34 % are melts, while, for the other compositions, the surface tension values correspond to the under-cooled liquid phase.

As expected, the surface tension increases with increasing nickel content. A good agreement was found between the values of this work and those recently obtained by container-less measurements,[9] in particular for the Al-rich compositions up to 68.5 % Al, with a difference less than 5 % which can be considered within the experimental uncertainty. On the other hand, the literature data[8] differed more than 8 %; however, not enough experimental details were provided in ref 8 for an explanation of the discrepancies to be found. The surface tension values of intermediate composition alloys correspond to the highest melting temperature alloys. The thermophysical properties of these alloys are very difficult to measure so that containerless methods, such as the levitated oscillating drop, were shown to be the most appropriate. To explain the behavior of the surface tension of the Al−Ni alloy as a function of composition, a correlation between surface tension and melting point has been applied,[9] on the basis of the relationship proposed in ref 11, derived for pure metals. However, no other evidence of such a correlation for binary systems is available in the literature. Therefore, the surface tension trend as a function of composition should be analyzed considering the strong tendency of the Al−Ni system to form intermetallic compounds, particularly in the intermediate composition range, where the effect of the contribution of short-range order phenomena is revealed to be strong.[12] In fact, since the structure of a liquid alloy is in some respects similar to that of a crystal,[13] at least at the melting point, compound formation can affect the surface tension behavior, reducing the segregation of the surface active component to the surface. This effect is shown to be more pronounced in the Ni-rich alloys, which are more influenced by the short-range order phenomena due to the closer compositional locations of the different intermetallic compounds. This phenomena can be well-described in the framework of the CFM model.[14] On the contrary, Al-rich alloys are much less influenced by the aforementioned phenomena, and thus their surface tension values agree better with corresponding values predicted by the RS model.[15] Butler's concept of a layered interface structure and the relationship between the component's activity in the bulk and the surface phase are basic hypotheses of both models.[14] It should be pointed out that in the framework of the CFM and the RS models mentioned above, the order energy parameters are determined from the thermodynamic data. Many details related to both models have been reported in refs 14 and 15. The main difference between the surface tension descriptions based on the two models arises from a different number of energy parameters, that is, four and one, respectively. Indeed, the effects of the chemical short-range order phenomenon on the surface properties of alloy melts can be described by the CFM model, while the use of the RS model allows estimation of such effects as a difference between the corresponding surface tension values, calculated by the two models.

Accordingly, a comparison between the experimental surface tension data at $T = 1673$ K and the values calculated by both the RS and the CFM formalisms are shown in Table 2.

Table 2. Experimental γ_{exp} and Calculated γ_{cal} Surface Tension Values at $T = 1673$ K[a]

alloy	γ_{exp}, this work / N·m^{-1}	γ_{exp}, from literature / N·m^{-1}	γ_{cal}, RS / N·m^{-1}	γ_{cal}, CFM / N·m^{-1}
$Al_{97.6}Ni_{2.4}$	0.746		0.763	0.763
$Al_{92.5}Ni_{7.5}$	0.758		0.780	0.784
$Al_{89.7}Ni_{10.3}$	0.854	0.855[8]	0.790	0.800
$Al_{87}Ni_{13}$	0.800		0.801	0.817
$Al_{76.5}Ni_{23.5}$	0.860		0.860	0.920
$Al_{75}Ni_{25}$	0.865	0.773[9]	0.865	0.940
$Al_{68.5}Ni_{31.5}$	0.926	0.877[9]	0.912	1.039
$Al_{11.4}Ni_{88.6}$	1.794	1.642[9]	1.653	1.801

[a] RS = regular solution model; CFM = compound formation model.

Table 3. Density ρ_L and Density Temperature Coefficient ρ' of Al−Ni Alloys at the Liquidus Temperature T_L

alloy	T_L / K	ρ_L / g·cm^{-3}	$\rho' \cdot 10^{-4}$ / g·cm^{-3}K^{-1}	ref
$Al_{76.7}Ni_{23.3}$	1340	3.72	−4.55	ref 9
$Al_{75}Ni_{25}$	1398	$(3.73 \pm 2.1)\cdot 10^{-4}$	−5.89	this work
$Al_{75}Ni_{25}$	1398	3.23	−4.20	calculated[11]
$Al_{75}Ni_{25}$	1398	3.53	−7.60	ref 16
$Al_{70}Ni_{30}$	1565	3.80	−9.40	ref 16
$Al_{68.5}Ni_{31.5}$	1620	$(4.08 \pm 3.2)\cdot 10^{-4}$	−13.3	this work
$Al_{68.5}Ni_{31.5}$	1620	3.43	−4.60	calculated[11]
$Al_{67.8}Ni_{32.2}$	1648	3.83	−7.37	ref 9

3.3. Density. To better characterize the properties of the Al_3Ni and AlNi alloys which were of main interest in the framework of IMPRESS project, the density was measured by applying the same methodology used for the determination of the surface tension described in Section 2.2. The density values were obtained from the ratio of the drop weight and the measured volume at each temperature during the large drop experiments. In Table 3, the experimental density values (ρ_L) of the $Al_{75}Ni_{25}$ and $Al_{68.5}Ni_{31.5}$ alloys at the liquidus temperatures (T_L) together with the temperature coefficients (ρ') are compared with calculated values as described in ref 11 and the literature data.[16,8]

The temperature density dependence in the temperature range investigated of both compositions can be fitted well by a linear function. Density behavior is shown to be consistent with the

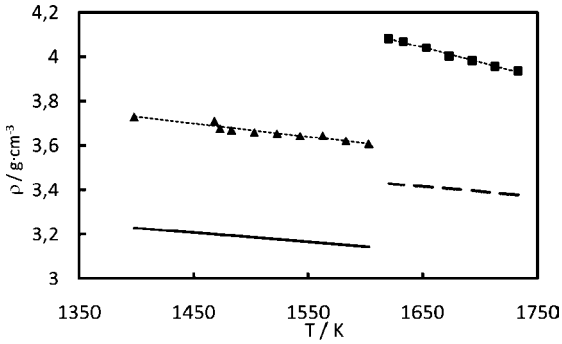

Figure 5. Density ρ of liquid Al−Ni alloys as a function of temperature T, measured under "oxygen-free" conditions (e.g., Ar 5 % H_2 + Zr getter atmosphere) and calculated by applying the ideal solution model:[11] ▲, $Al_{75}Ni_{25}$; ■, $Al_{68.5}Ni_{31.5}$. Dotted lines, •••, linear fit to the data. Calculated linear relationships: continuous line, —, $Al_{75}Ni_{25}$; broken line, - - -, $Al_{68.5}Ni_{31.5}$.

alloy composition: it increases with increasing Ni content in the alloy. A fairly good agreement exists between the density values measured in this work and the data available in the literature,[8,16] in particular data obtained by a containerless method by an electromagnetic levitation facility designed for optical dilatometry. In Figure 5, the density experimental values as a function of temperature are shown together with the relationships evaluated by applying Vegard's rule[12] for ideal solutions. The experimental densities differ up to 16 % from the corresponding calculated values. This latter evidence is not surprising considering the already mentioned compound-forming tendency of the Al−Ni system. The presence of chemical ordering induces an increase of the actual density value as investigated by other authors, in particular relating the excess volume phenomena with density and atomic volume.[16]

4. Conclusion

The surface tension of a set of Al−Ni alloys was determined by the large drop technique. The density of two intermetallic compounds, AlNi and Al_3Ni, was also determined by the same method.

The experimental results agree well with recent literature data and can be explained by the tendency of these alloys to form intermetallic compounds. In particular, the behavior of Ni-rich alloys is well-described in the framework of the CFM model, able to describe the influence of the short-range order phenomena due to the presence of several intermetallic compounds. The thermophysical properties data of the Al-rich alloys measured in this work agree better with the predictions derived from the application of the RS model due to the weak influence of the intermetallics.

Acknowledgment

Special thanks to Tiziana Lanata (CNR-IENI Genoa) and Simona Delsante (DCCI, University of Genoa) for part of the experimental work and Marco Pini (CNR-IENI Lecco) for technical assistance.

Literature Cited

(1) Jarvis, D. J.; Voss, D. IMPRESS Integrated Project—An overview paper. *Mater. Sci. Eng., A* **2005**, *413*−*414*, 583–591.
(2) Massalski, T. B.; Murray, J. L.; Bennet, K. H.; Baker, H. *Binary Alloy Phase Diagrams*; American Society for Metals: Metals Park, OH, 1986.
(3) Flagan, R. C.; Lunden, M. M. Particle structure control in nanoparticle synthesis from the vapor phase. *Mater. Sci. Eng., A* **1995**, *204*, 113–124.
(4) Ricci, E.; Arato, E.; Passerone, A.; Costa, P. Oxygen tensioactivity on liquid-metal drops. *Adv. Colloid Interface Sci.* **2005**, *117* (1−3), 15–32.
(5) Knacke, O.; Kubashewski, O.; Hesselmann, K. *Thermochemical properties of inorganic substances*, 2nd ed.: Springer Verlag: Duesseldorf, 1991.
(6) Aune, R.; Battezzati, L.; Egry, I.; Etay, J.; Fecht, H. J.; Giuranno, D.; Novakovic, R.; Passerone, A.; Ricci, E.; Schmidt-Hohagen, F.; Seetharaman, S.; Wunderlich, R. Surface Tension Measurements of Al-Ni Based Alloys from Ground-Based and Parabolic Flight Experiments: Results from the Thermolab Project. *Microgravity Sci. Technol.* **2005**, *XVIII* (3/4), 73–76.
(7) Maze, C.; Burnet, G. A non-linear Regression method for calculating surface tension and contact angle from the shape of sessile drop. *Surf. Sci.* **1969**, *13*, 451–470.
(8) Ayushina, G. D.; Levin, E. S.; Gel'd, P. V. The density and surface energy of liquid alloys of aluminium with cobalt and nickel. *Russ. J. Phys. Chem.* **1969**, *43* (11), 1548–1551.
(9) Egry, I.; Brillo, J.; Holland-Moritz, D.; Plevachuk, Yu. The surface tension of liquid aluminium-based alloys. *Mater. Sci. Eng., A* **2008**, *495*, 14–18.
(10) Cummings, D.; Blackburn, D. Oscillations of magnetically levitated aspherical droplets. *J. Fluid Mech.* **1991**, *224*, 395–416.
(11) Iida, T.; Guthrie, R. I. L. *The Physical Properties of Liquid Metals*; Clarendon Press: Oxford, 1993.
(12) Witusiewicz, V. T.; Arpshofen, I.; Seifert, H. J.; Sommer, F.; Aldinger, F. Thermodynamics of liquid and undercooled liquid Al-Ni-Si alloys. *J. Alloys Compd.* **2000**, *305*, 157–171.
(13) Frenkel, J. *Kinetic Theory of Liquids*; Clarendon Press: Oxford, 1946.
(14) Singh, R. N. Short-range order and concentration fluctuations in binary molten alloys. *Can. J. Phys.* **1987**, *65*, 309–325.
(15) Guggenheim, E. A. *Mixtures*; Oxford University Press: London, 1952.
(16) Plevacuk, Yu.; Egry, I.; Brillo, J.; Holland-Moritz, D.; Kaban, I. Density and atomic volume in liquid Al-Fe and Al-Ni binary alloys. *Int. J. Mater. Res.* **2007**, *02*, 107–111.

Received for review December 15, 2009. Accepted April 17, 2010. The work presented here was funded by the European Commission under Contract FP6-500635-2.

JE901055J